Natural Hazards
https://doi.org/10.1007/s11069-024-06512-5

ORIGINAL PAPER

Performance of CA_Markov and DINAMICA EGO models to evaluate urban risk in Antofagasta and Mejillones, Chile

Cristian Henríquez[1,2,3] · **Robert Gilmore Pontius Jr.**[4] · **Paulina Contreras**[1]

Received: 13 June 2023 / Accepted: 16 February 2024
© The Author(s), under exclusive licence to Springer Nature B.V. 2024

Abstract
The rapid growth of cities worldwide is a phenomenon that has generated numerous debates about the effects it could have on the environment and society. An issue that has not been well addressed in the literature is the relationship between expected urban growth and risks to natural hazards. The relationship is an important aspect for planning because urban expansion is uncertain. In this sense, land change simulation models can be useful tools to address this uncertainty, because simulation models can produce growth scenarios, which allow anticipation of exposure to natural threats. This article compares two land change simulation models: the CA_Markov model in the Selva version of IDRISI and the DINAMICA EGO model. We apply both models to extrapolate areas of future urban gain in the coastal cities of Antofagasta and Mejillones, where there is high exposure to tsunamis, mudslides, and steep slopes. The models can extrapolate differently in terms of both quantity and spatial allocation of urban gain depending on the parameter settings. CA_Markov projected urban growth adjacent to existing urban patches, while best fits to Markov equation, and the urban form was achieved with DINAMICA EGO, according to our parameter settings. We conclude that if modelers understand the models' behaviors, then applying these spatially explicit models to natural risks opens great prospects for urban planning and risk management, especially in countries highly exposed to dangerous natural events, such as in the case of Chile.

Keywords Land use change model · Atacama desert · Natural risk · Urban planning

✉ Cristian Henríquez
cghenriq@uc.cl

Robert Gilmore Pontius Jr.
rpontius@clarku.edu

Paulina Contreras
plcontreras@uc.cl

[1] Instituto de Geografía, Pontificia Universidad Católica de Chile, Santiago, Chile

[2] Centro Interdisciplinario de Cambio Global, Pontificia Universidad Católica de Chile, Santiago, Chile

[3] Centro de Desarrollo Urbano Sustentable ANID/FONDAP, Santiago, Chile

[4] School of Geography, Clark University, Worcester, MA, USA

Published online: 03 April 2024

1 Introduction

There is unprecedented growth in urban areas worldwide. In 2008, for the first time in history, more than 50% of the population was living in urban areas while urban population is expected to rise steadily over time (United Nations 2019). The United Nations (2019) estimates that by the year 2050, this percentage will reach 86% in Latin America. In Chile, 88% of the population resides in urban areas, and the northern regions of the country exceed 91% (INE 2018).

One of the main problems with this accelerated urban growth is that it has not been well planned or has been completed in a reactive and partial way. In many cases, slow approval of urban planning tools makes it impossible to anticipate rapid real-estate development dynamics or the occurrence of spontaneous and irregular settlements, and informal housing. This creates a serious problem when the city expands in a fragmented and sprawling form outside the official city limits, especially over natural hazard zones, increasing the risk of natural disasters. This causes an increase in exposure of the population to risk. In the particular case of developing countries, this can increase vulnerability of the poorest population and decrease the ability of the precarious urban infrastructure to cope with extreme events (Bozzolan et al. 2020; Depicker et al. 2021; Dille et al. 2022; Raju et al. 2022; Ozturk et al. 2022; Veerbeek and Denekew 2011).

Various authors (Trentin et al. 2010; National Research Council 2014; Henríquez 2014) mention that this accelerated growth of cities requires new analytical methodologies that can better manage the planning process. Some of the new methodologies are land change simulation models. The ability to understand, characterize, measure, and simulate the dynamics of urban land change provides great benefits for decision makers (Agarwal et al. 2002; National Research Council 2014). The integration of GIS, remote sensing, and environmental modeling has led to enormous advances in the generation of future scenarios and evaluation of environmental impacts (Weng 2001a, 2001b; Pijanowski et al. 2002; Huong and Pathirana 2013), transportation (Waddell 2011; Pozoukidou 2014), regional planning (Kuijpers-Linde 2011; Jacobs et al. 2011) and the land market (Dekkers and Rietveld 2011). Few applications evaluated natural risks (Chen et al. 2001; Zerger 2002; Martins et al. 2012). Some models allow heuristic simulation based on expert opinion and integrate MultiCriteria Evaluation (MCE) with techniques such as the Markov chain analysis and cellular automata. Other models incorporate techniques such as weight of evidence algorithm. An example of the first case is the CA_Markov model (Clark Labs 2012), and an example of the second case is the DINAMICA EGO model (Soares-Filho et al. 2002).

Knowing what the implications are of urban growth on natural risks is an urgent need, especially in countries such as Chile that have high exposure to natural hazards such as earthquakes, tsunamis, tides, and landslides, among others. This paper aims to answer the question: How will future urban growth influence exposure to natural hazards in Antofagasta and Mejillones, Chile? Our study applies two simulation models of urban land use change to determine the future risk of the cities of Antofagasta and Mejillones. The two models are CA_Markov (Clark Labs 2012) and DINAMICA EGO (Soares-Filho et al. 2002). We determine the major natural threats that affect cities by considering the hazards from tsunamis and mass movements. Then, we incorporate the forcing factors of urbanization into the models to simulate urban growth. Finally, we combine the results to evaluate future exposure to natural threats.

The manuscript is structured in 5 parts: the first part reviews the framework of natural hazards in Chile; then the methodology of the two spatially explicit models used

(CA_Markov and DINAMICA EGO) is explained; next, the results of the urban simulations are presented; then the implications of the results on territorial risk management are discussed; finally, the conclusions are presented.

2 Natural threats in northern Chile

Most cities in Chile, especially the coastal cities, are subject to substantial exposure to extreme natural hazards. In particular, coastal cities in the Antofagasta region are exposed to a permanent seismic risk, and therefore, also to the threat of tsunamis. In general, these cities present topographic, geological, and climatic characteristics that trigger intense and violent mass movement processes (Hauser 1997).

Major threats include tsunamigenic earthquakes that are concentrated mainly in the Pacific Ocean basin, in what is known as the "Pacific Ring of Fire". Chile is located on the edge of an active subduction, therefore Chile experiences 74% of seismic activity in South America (Pararas-Carayannis 2010). In particular, the north of Chile is a seismically active zone where the 1877 earthquake occurred, whose magnitude was estimated to be close to 8.3 Mw (Pritchard and Simons 2002).

More recent events include the 2007 earthquake with the epicenter in Tocopilla having a magnitude of 7.7 M_w (Béjar-Pizarro et al. 2013), and the 8.2 M_w earthquake in Iquique on April 1, 2014 (Barrientos 2014). This last event partially changed the trajectory for the north of the country. According to the National Seismological Service of Chile, the northern seismic gap was divided into three seismic zones. The first is located to the north of the rupture zone of the earthquake, between the towns of Ilo in Peru and Cuya in Chile. This first zone has a length of approximately 200 km and has remained a seismic gap. The second zone is in the 2014 earthquake zone between Pisagua and Punta Patache, which did not release all of the energy from the superficial part of the fault. The third zone, also a seismic gap, is between the towns of Punta Patache and Tocopilla-Mejillones (Barrientos 2014). This would cause two seismic events in the north of the country. The first is where the seismic gaps to the north and south of the 2014 rupture zone would generate earthquakes with an approximate magnitude of 8.2 M_w The second possibility is where both seismic gaps would be simultaneously activated, generating an event exceeding 8.5 M_w (Hayes et al. 2014; Schurr et al. 2014). This means that cities such as Antofagasta and Mejillones could be exposed to a possible seismic event of no less than 8.2 M_w. These types of events also expose the zone to tsunamis.

Regarding these types of events, the tsunamis that occurred in southern Chile in 1960 were linked to the world's largest earthquake with a magnitude of 9.0 M_w, and the 2010 tsunami from the 8.8 M_w earthquake that struck south-central of the country from the Arauco Peninsula to Pichilemu (Barrientos 2014; Pararas-Carayannis 2010). The north of the country has not experienced a tsunami of large-scale proportions in recent years. According to the Oceanographic Service of the Chilean Navy (SHOA), based on a worst-case scenario of a magnitude 9 M_w event, the north and especially the south of the urban area of Antofagasta would expect dangerous tsunami heights. In the case of Mejillones, flood levels are estimated to be more than six meters, which would cover almost the entire urban area. That simulation was based on the historical event of 1877 (SHOA 2012, 2013), which was an approximate 8.3 M_w earthquake.

Finally, other dangerous events are mass movement processes. The north of Chile has one of the driest deserts in the world. Scarce vegetation cover, steep slopes, low

precipitation, and intensity of earthquakes make this territory highly exposed to events such as flooding, mudslides, debris flow, rockfall, and coastal cliff landslides. For example, an extreme precipitation event in March 2015 in the Atacama Desert caused damaging stream flows due to precipitation greater than 45 mm (Henríquez et al. 2019). There were 18 floods and overflows of watercourses and mudslides (ONEMI 2015a, 2015b). A low-pressure system combined with unusual oceanic and atmospheric conditions produced a heavy precipitation event (Barrett et al. 2016). This event generated catastrophic disasters (Barrett et al. 2016; Wilcox et al. 2016), with 31 deaths, 16 missing persons, 30,000 displaced persons, 164,000 people affected, and widespread damage to homes, roads, bridges, and railways (ONEMI 2015a, 2015b).

This research includes the cities of Antofagasta and Mejillones located in the northern coastal plain between latitudes 23°00′ S and 23°03′ S, and longitudes 70°17′ W and 70°37′ W, Antofagasta region (see Fig. 1). The city of Antofagasta is the fifth largest city in Chile and has experienced rapid growth linked to mining. Mejillones is located close to Antofagasta as it is an important industrial city port. Both cities have been chosen since they present little information on risk management and urban growth.

The city of Antofagasta is located on a narrow marine abrasion plain between the Coastal mountain range and the Pacific Ocean. The city's average width varies between 2.5 and 3.0 km, and its length from north to south reaches 16 km. The Coastal mountain range consists of a chain of eroded hills that rise abruptly in elevation, reaching up to 1300 m. This city is the capital of the II region of Antofagasta with 348,517 inhabitants (INE 2018) and strong urban growth towards hillsides (Fig. 2) and north and south sectors. Lately, Antofagasta is experiencing immigration of people who come in search of better job opportunities associated with copper mining activities.

The town of Mejillones is in the Bay of Mejillones on an extensive coastal plain. The city of Mejillones has 12,784 inhabitants and its main economic activities are port and industrial activities. Both cities have copper mining as their main economic activity.

Both cities are in the Atacama Desert, which has an extremely dry climate. According to the Köppen-Geiger classification system, Antofagasta has a cold desert climate (BWk) with an average of 1.7 mm/year and Mejillones has a warm desert climate (BWh) (Sarricolea et al. 2017).

The Intercommunal Regulatory Plan of coastal border land use of the Antofagasta Region (SEREMI MINVU 2004) identifies areas at risk from steep slopes, especially in the Coastal mountain range. In Antofagasta, the most severe disaster was a mudslide that occurred in the early hours of June 8, 1991 (Hauser 1997). A sudden and violent rainfall, between 17 and 47 mm, caused mudslides and flooding. The city was declared a disaster zone. There were 91 dead, 16 missing, 715 injured, 65,000 homeless, and 190,000 affected (Vargas et al. 2000). The disaster caused US$ 70.000.000 in losses, 600 homes were destroyed and 6,000 homes were affected, becoming the most-costly disaster for the city (La Red/DesInventar 2009). Garreaud and Rutllant (1996) state that the extraordinary precipitation of 24 mm/hr that caused the event of 1991 has a return period of 100 years. Nevertheless, Vargas et al. (2000) assert that the return period of these types of events is 30 years. In the twentieth century, at least six events exceeding 20 mm/hr were identified when at least four mudslides occurred (Vargas et al. 2000). All of these events are closely related to heavy rainfall events associated with ENSO (INE 2013; NOAA 2014; Vargas et al. 2000).

This background demonstrates that these types of events are recurrent and have affected the entire coastal section near the city of Antofagasta. During June 6–7, 2017 there was heavy rainfall of 20.6 mm in Antofagasta. The historical mudslides and

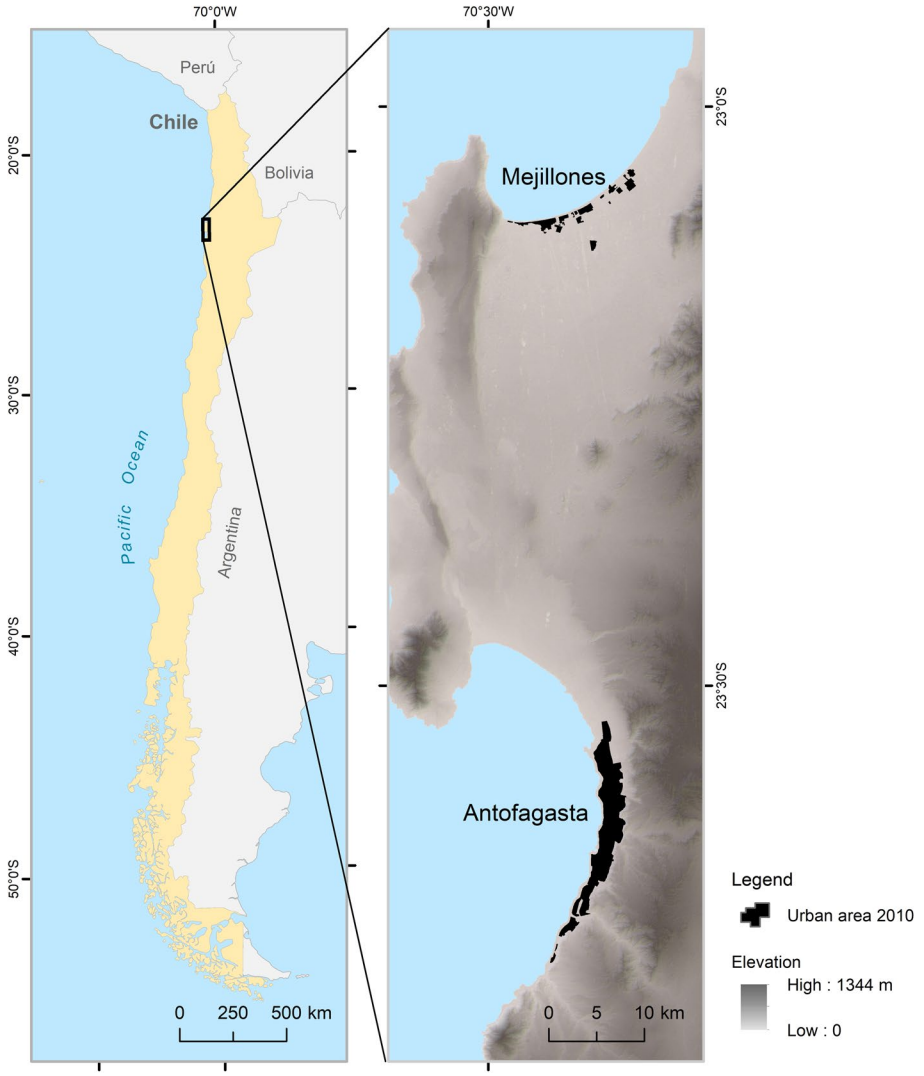

Fig. 1 Study area

landslides deposits identified by Vargas et al. (2000), the deposits from the 1991 mudslide identified by Hauser (1997), and the risk studies completed in the last revision of the Municipal Regulatory Plan (MRP) of Antofagasta (Ilustre Municipalidad de Antofagasta 2012) show the fragility of the urban system.

In Mejillones, the landslide risk is lower because the Coastal mountain range is further away, nonetheless, the MRP identifies potential risk zones (Ilustre Municipalidad de Mejillones 2013). In addition, the city is fully exposed to tsunamis due to its position in the bay. Therefore, both cities could expect a high level of exposure in the future. This translates into a high level of risk for the population and the infrastructure, especially in light of the rapid growth dynamics of these cities.

Fig. 2 Urban growth of Antofagasta city over Coastal mountain range

3 Materials and methods

3.1 Materials

The land use maps were extracted from Landsat satellite images and the Thematic Mapper sensor for the years 1990, 2000, and 2010. Land use was classified visually using false color compositions, bands 742 in RGB, and historical maps of the zone as reference (Hauser 1997; Vargas and Ortlieb 1997; Vargas et al. 2000). For each year, we produced a map of two categories: urban and non-urban. If a pixel is urban at a particular time point, then the pixel remains urban at all subsequent time points. The definition of urban is industrial, commercial, residential, or recreational uses. Figure 3 shows that almost all urban growth in Antofagasta occurs adjacent to existing urban patches, while a substantial portion of urban growth in Mejillones derives from patches that are not connected to existing urban patches. The size of urban growth accelerated from 1990–2000 to 2000–2010 in both cities.

Also included in the analysis is the urban boundary cover that is defined by the Municipal Regulatory Plans existing in both cities (Ilustre Municipalidad de Antofagasta 2012; Ilustre Municipalidad de Mejillones 2013) and Regional Secretariat of the Ministry of Housing and Urbanism of Antofagasta (SEREMI MINVU 2004). All coverage was digitized and georeferenced in ArcGIS 9.3. Cell size for GIS analysis is 10-by-10 m.

We compiled materials concerning the major factors of urban land use change, which we drew from the literature review (Huong and Pathirana 2013; Mahiny and Clarke 2012; Pijanowski et al. 2002; Puertas et al. 2014; Trentin et al. 2010; Weber and Puissant 2003) and expert consultations from the Regional Secretariat of the Ministry of Housing and Urban Planning of Antofagasta (SEREMI MINVU). We included slope & elevation, and also proximity factors such as distance to roads, shoreline, city center, and sanitary facilities. Table 1 summarizes these factors.

3.2 Methods

Each land use model, CA_Markov and DINAMICA EGO, was run for a single box that includes the two cities.

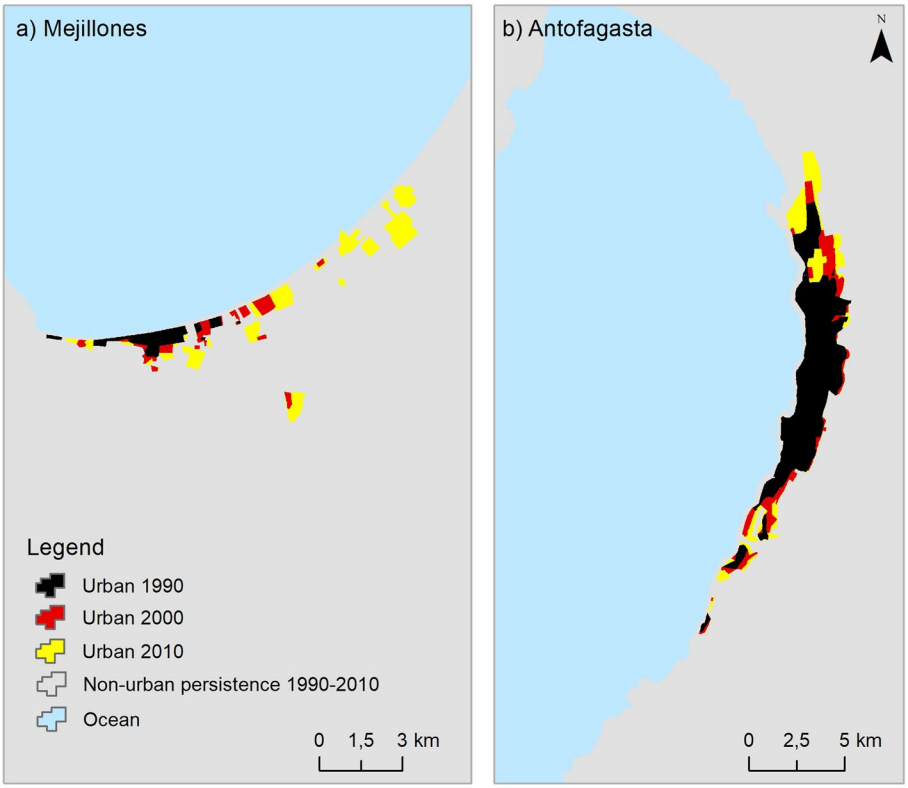

Fig. 3 Urban growth in Antofagasta and Mejillones across two decades

Table 1 Description of urban driving forces

Driving forces	Unit	Source	Year
Elevation	m	ASTER global Digital Elevation Model v.2	2011
Slope	%	ASTER global Digital Elevation Model v.2	2011
Distance to main roads	m	SEREMI MINVU and MRP	2008–2012
Distance to shoreline	m	SEREMI MINVU and MRP	2008–2012
Distance to CBD	m	SEREMI MINVU and MRP	2012
Distance to sanitary facilities	m	Antofagasta Superintendent of Water and Sanitary Services	2013

3.2.1 CA_Markov model

We used the CA_Markov model in the Selva version of the GIS software IDRISI (Clark Labs 2012). We simulated the single transition from non-urban to urban. Figure 4 shows the flows of information in CA_Markov for two runs. The first run uses 1990 and 2000 as the calibration interval to extrapolate to the 2000–2010 validation interval. A validation procedure compares the simulated urban growth to the actual urban growth during

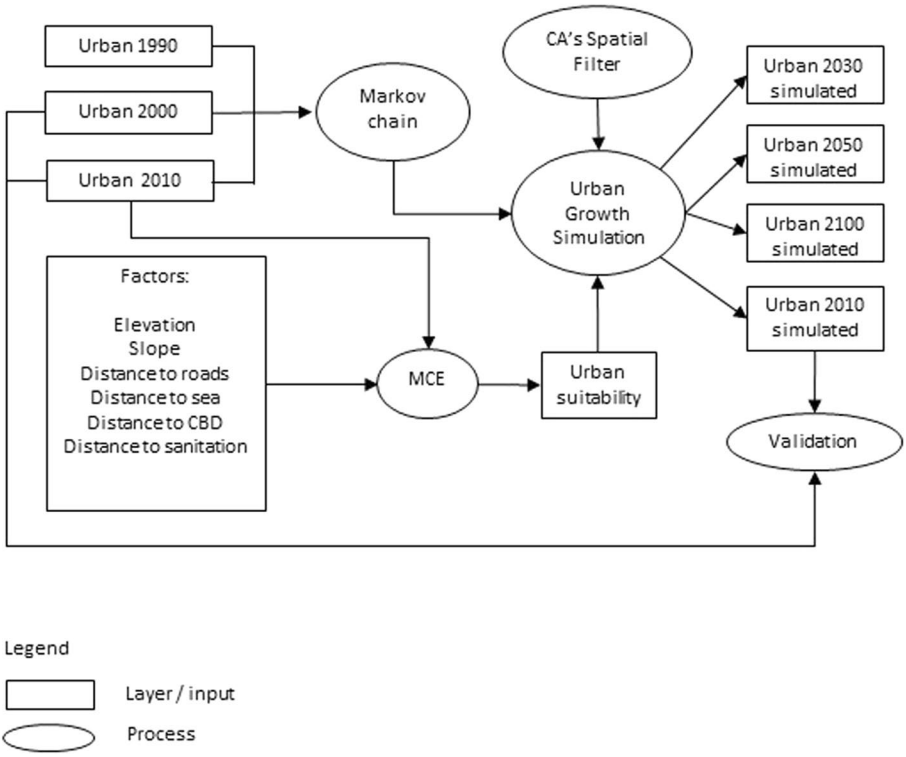

Fig. 4 CA_Markov model

2000–2010. The second run uses 1990 and 2010 as the calibration interval to extrapolate during three sequential time intervals: 2010–2030, 2030–2050, and 2050–2100.

Any land change simulation model must specify two types of information called quantity and allocation. For our case study, quantity concerns the size of urban growth during each time interval; allocation concerns the spatial distribution of the urban growth across the map. A CA_Markov model uses a Markov chain to specify the quantity and then uses Cellular Automata to determine the allocation of the specified quantity.

A Markov chain extrapolates the size of urban through time in a trajectory equivalent to Eq. (1), which uses the following notation. $U(Y_t)$ is the size of urban area at year Y_t of time point t where $t=0, 1, 2, \ldots$ The calibration time interval is from Y_0 to Y_1. E is the size of the extent, which is the constant union of urban and non-urban areas at any time point. The size of the extent depends on how the user defines the non-urban size at Y_1. Larger non-urban sizes cause slower extrapolations. The ratio in the square brackets is a constant Markov proportion, which is in the interval (0, 1) because $0 < U(Y_0) < U(Y_1) < E$. As Y_t increases, $U(Y_t)$ increases at a decelerating area per year asymptotically towards E.

$$U(Y_t) = E - [E - U(Y_0)] \left[\frac{E - U(Y_1)}{E - U(Y_0)} \right]^{\{[Y_t - Y_0]/[Y_1 - Y_0]\}} \quad (1)$$

The Cellular Automata part of IDRISI's CA_Markov model has two parts (Clark Labs 2012). The first part is a spatial filter that constrains the urban growth to be within a particular distance of existing urban pixels. The size of the filter dictates the particular distance. We used a spatial filter of size eight and a filter shape of the Moore's neighborhood. Cellular Automata's second part is a MCE, which uses a weighted combination of the five factors in Table 1. Table 2 and Fig. 5 shows how we used a fuzzy membership function to standardize each factor depending on its relationship with urban growth. The fuzzy functions derived from discussions with the regional planning team of the MINVU Regional Secretariat.

An analytic hierarchy process (AHP) weighted each factor based on expert opinion (Saaty 1980). Professionals from the MINVU Regional Secretariat compared the importance of each pair of factors according to a scale from 1/9 to 9. The AHP computed that the distance to sanitary facilities is the most important variable (43%) and especially in extremely arid regions. Second is the distance to main roads (24%). AHP applies smaller weights to distance to CBD (11%), distance to the shoreline (10%), slope (7%), and elevation (5%). Then, the normalized and weighted factors are added to produce a map of suitability that guides the spatial allocation of simulated urban growth.

3.2.2 DINAMICA EGO model

The DINAMICA EGO model was developed by the Centro de Sensoriamento Remoto da Universidade Federal de Minas Gerais—CSR/UFMG, Brazil. DINAMICA EGO's documentation claims that the model uses a Markov chain to extrapolate the quantity of urban growth, which implies that urban growth would decelerate in terms of area per year according to Eq. (1). DINAMICA EGO simulates the spatial allocation by using cellular automata and transition probability maps that are based on the weights of evidence and a genetic algorithm (Mas et al. 2012). The simulation process works iteratively to model any type of transition, as well as encompass any duration of time and any number of time intervals (Soares-Filho et al. 2002: 233). This model is based on three main stages: the calculation of a land use transition matrix, weights of evidence to create a probability map, and the application of cellular automata and spatial stochastic feedback (patcher and expander) during each time increment of the simulation (Soares-Filho et al. 2002). Figure 6 shows the flow of information in DINAMICA EGO.

First, the transition matrix depicts the quantity of change in a system of discrete time increments, where the number of pixels of urban growth during an increment is a fixed percentage of the number of non-urban pixels at the beginning of the time increment (Soares-Filho et al. 2009). Like with the CA_Markov applications, the first model run has calibration during 1990–2000 and validation during 2000–2010, while the second model run has calibration during 2000–2010 and extrapolation during 2010–2030, 2030–2050, and 2050–2100.

In the second stage of modeling, the same factors identified in the CA_Markov model are used. DINAMICA EGO uses weights of evidence (WoE) to combine the factors into a probability map. WoE is a Bayesian inference method that identifies the posterior probability of an occurrence of an event according to a spatial test pattern (Ferreira et al. 2013). This process allows the revision and modification of the results based on expert opinion (Pérez-Vega et al. 2012; Ferreira et al. 2013; Mas et al. 2012). Therefore, the WoE were partially modified to improve the model adjustment by leveraging the analytical hierarchy analysis used in the MCE of the CA_Markov model. The transition matrix is transformed

Table 2 Fuzzy parameters

Factors	Fuzzy set membership function	Membership function shape	Control points				Unit	Description
			a	b	c	d		
Elevation	Sigmoidal	Monotonically decreasing	–	–	51.49	632	Meters	DEM and normative analysis (MRP)
Slope	J-Shaped	Monotonically decreasing	–	–	10.24	29.2	Percentage	Slope Analysis
Distance to main roads	Linear	Monotonically decreasing	–	–	400	2300	Meters	Euclidean distance analysis
Distance to shoreline	Linear	Symmetric	20	40	120	27,416	Meters	Normative analysis (Article 594 Civil Code and MRP)
Distance to CBD	J-Shaped	Symmetric	200	900	1100	3500	Meters	Euclidean distance analysis
Distance to sanitary facilities	Sigmoidal	Monotonically decreasing	–	–	0	27,275	Meters	Euclidean distance analysis

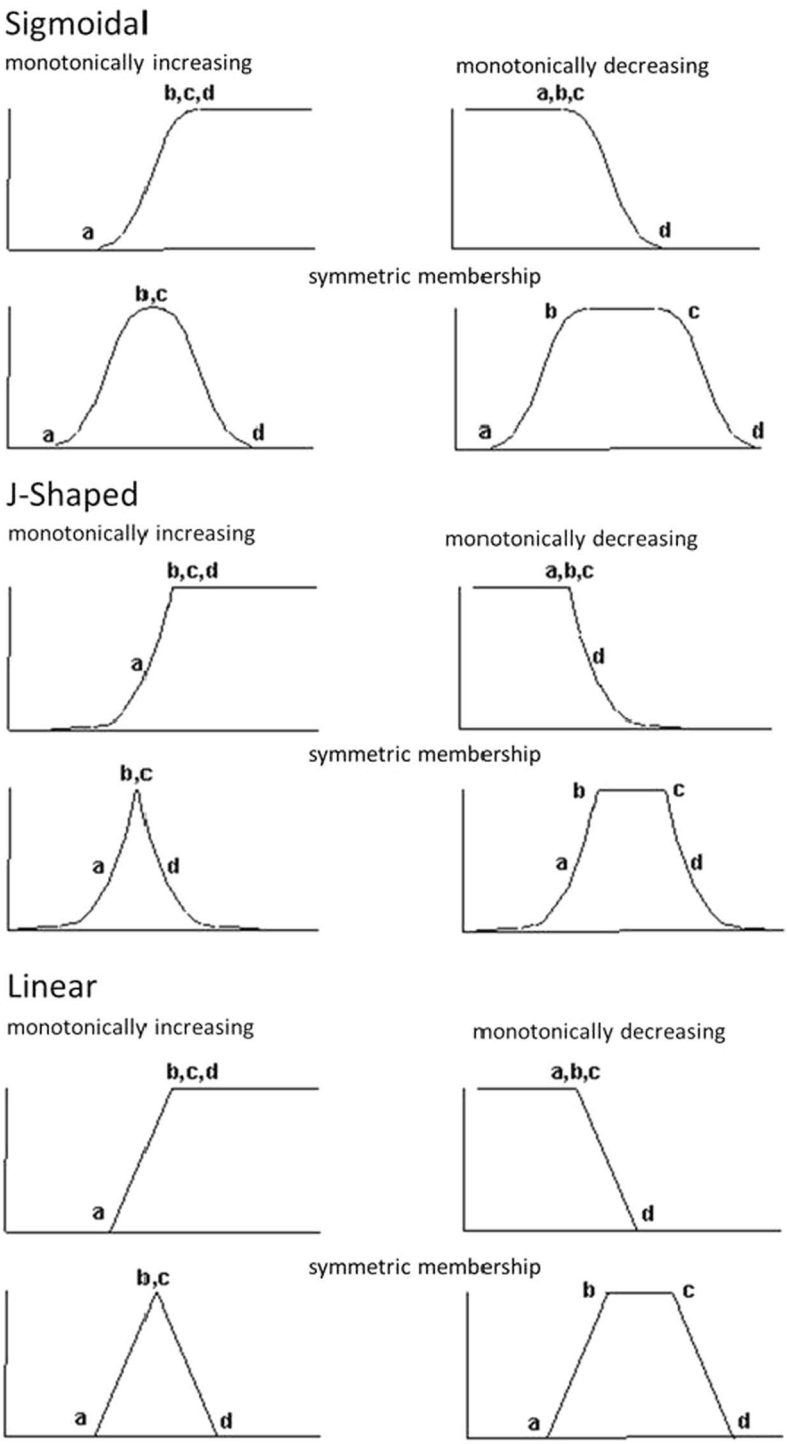

Fig. 5 Fuzzy set membership functions. Source: Clark Labs (2012)

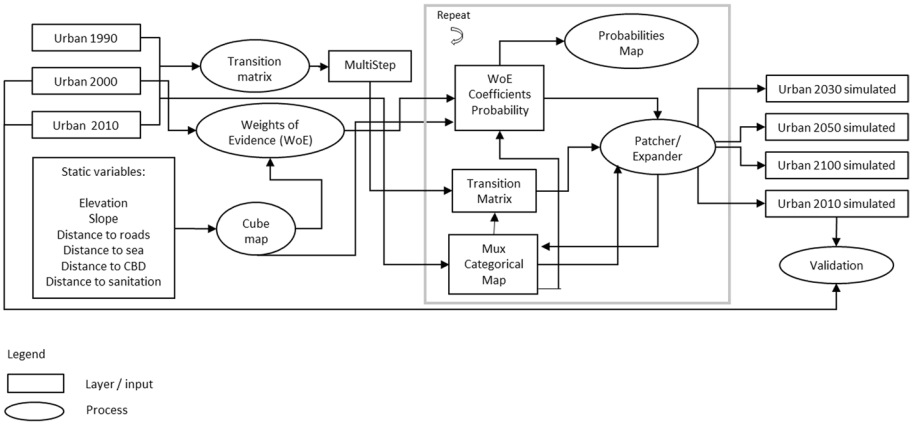

Fig. 6 DINAMICA EGO model and submodel

into an annual transition rate to project the changes on an annual basis by applying a matricial calculation.

In the final stage of the modeling process, the model uses two complementary transition functions: Patcher and Expander (Mas et al. 2012; Soares-Filho et al. 2002). The first function creates new patches through a seeding mechanism, while the second focuses on stochastic expansion processes of the existing patches. The Patcher option was used to differentiate the urban growth pattern from the result obtained from the CA_Markov model, that is, to generate more patches on the periphery of the consolidated urban area. A model with the Expander option was also developed to compare the performance of the urban shape and size in relation to the other models in the calibration phase. The patch isometry, and patch mean, and variance were established according to the pattern of real changes in the calibration period (Garcia-Alvarez 2018), using the FRAGSTAT program (McGarigal et al. 2015) as support. In addition, the simulation used the corroded probabilities option to test the difference between the amount of change according to the Markov method and cellular automata.

3.3 Validation method

The calibration time interval is 1990–2000 for the method to compare the simulated change to the reference change during the 2000–2010 validation time interval. The simulation includes distance to main roads and distance to sanitary facilities as independent variables. Those two variables are from after 2010; however, many of those roads and facilities existed before the start of the validation time interval. The validation derives from the methodology proposed by Pontius Jr et al. (2008, 2011, 2018) and illustrated by several others (Liu et al. 2014; Varga et al. 2019). This validation method compares three maps of urban versus non-urban: the reference map at 2000, the reference map at 2010, and the simulation map at 2010. The misses, hits, and false alarms show how the reference change compares to the simulated change (Pontius Jr 2022). Misses are errors due to reference urban growth simulated as persistence. Hits are correct due to reference urban growth simulated as urban growth. False Alarms are errors due to reference persistence simulated as urban growth.

3.4 Future threats

We overlaid the simulated urban growth with maps of the risks of three types of natural hazards: Tsunamis, Mudslides, and Steep Slopes. The tsunami risk map comes from the Hydrographic and Oceanographic Service of the Chilean Navy (SHOA 2012). The mudslides risk map derives from the Land-Use Planning Instruments (LUPI) and previous studies (Hauser 1997; Vargas et al. 2000). The steep slopes map derives from LUPI and the Intercommunal Regulatory Plan of coastal border land use of the Antofagasta Region (SEREMI MINVU 2004; Ilustre Municipalidad de Antofagasta 2012; Ilustre Municipalidad de Mejillones 2013).

4 Results

4.1 Reference data and simulation outputs

Figure 6 shows how the two models simulate the urban size of each city during three time intervals: 2010–2030, 2030–2050, and 2050–2100. For each series in Fig. 7, if the slope during a time interval is steeper than the slope during the previous time interval, then the urban growth has accelerated across the two time intervals; if the slope during a time interval is flatter than the slope during the previous time interval, then the urban growth has accelerated across the two time intervals. Each model applied to each city shows that urban growth accelerates across some time intervals and decelerates across other time intervals.

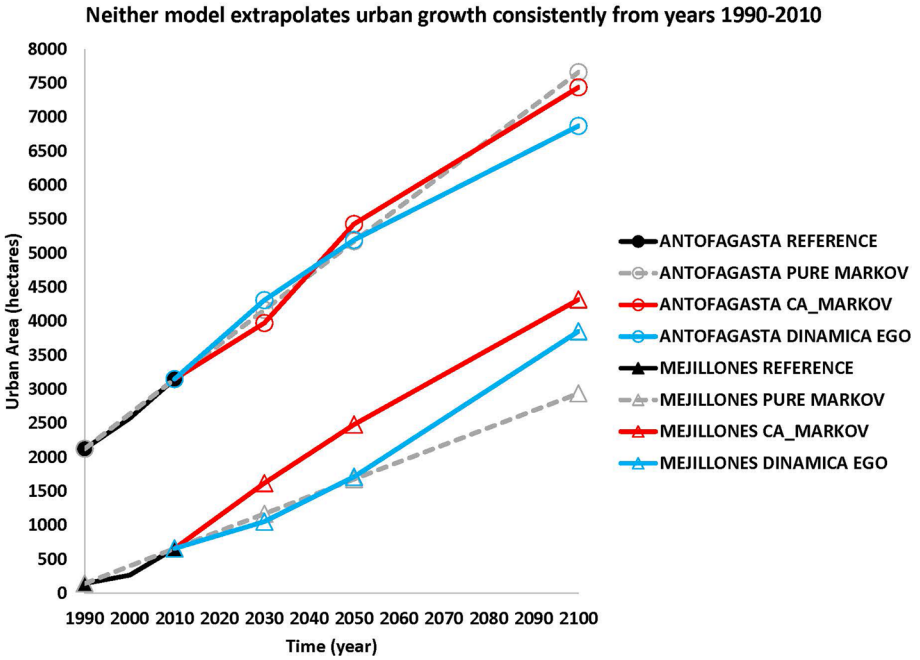

Fig. 7 Extrapolation of the quantity of urban growth based on the 1990–2010 calibration time interval

Each city has a dashed line that interpolates Eq. (1) through the urban area at 2000 and 2010. If the models would have extrapolated the quantity according to a Markov chain, then the extrapolation would match the dashed line. Results show that neither model follows a pure Markov chain.

Figure 8 shows how each model allocates the quantity of urban growth. Growth occurs near the interior of Mejillones. In Antofagasta, growth is allocated along the coast. Inclusion of the spatial filter causes the CA_Markov model to allocate a ribbon of urban growth near the edges of existing urban areas. DINAMICA EGO allocates some of the urban growth as a leap-frog pattern.

Table 3 links the simulated urban areas with the areas of natural hazards, which reveals a clear trend towards increased exposure. For the year 2010 in Antofagasta, 1336 hectares are exposed to natural disasters, 83% of which are mudslides. In Mejillones, the main threat is the tsunami with 200 ha exposed, which is equivalent to nearly 100% of all existing threats in the city. When compared to the year 2100, the simulations in CA_Markov and DINAMICA EGO show that exposure to natural hazards is extrapolated to increase between 722 and 580% from 2010. For both models, the most important hazard is Mudslide, then steep slope, and finally tsunami (Table 3; Fig. 7).

In Mejillones, the threat of a tsunami is most prominent in the city and will increase to 312 ha by 2100. The mass movements turn more relevant, from 1.5 ha in 2010 to almost 30 ha in 2100. The areas of steep slope become especially important because steep slope does not register in 2010 but is expected to reach 79 ha in 2100.

In both Antofagasta and Mejillones, urban growth is projected outside the current urban boundary (Plan Regulador Comunal and Intercomunal, see Fig. 7). In Antofagasta, 9 ha is outside the urban limits for 2030, which increases to 30 ha by 2050 and 130 ha by 2100. By 2030 in Mejillones, an estimated 75 ha outside the urban limits is exposed to the threat of steep slopes, which increases to 1193 ha in 2100.

4.2 Validation

Figure 9 shows the calibration and validation of the quantity of urban growth. Both cities experience accelerating urban growth according to the reference data across two decades. Therefore, the reference data do not follow a Markov chain because a Markov chain does not extrapolate accelerating growth from the calibration interval to the validation interval. The dashed lines show how a pure Markov chain calibrated during 1990–2000 extrapolates during 2000–2010 according to Eq. (1). Neither simulation model generates simulated maps that portray a pure Markov chain. We set the parameter for proportional error to 0.15 in the Markov module of the CA_Markov model based on the recommendation of IDRISI's documentation. It would have been helpful for the documentation to describe more clearly the effect of a positive parameter for proportional error, which is to increase the size of the simulated change beyond what a pure Markov chain would extrapolate. Consequently, CA_Markov simulates more urban growth than DINAMICA EGO, which allows for an insightful comparison between the validation of models that vary in the quantity of simulated change.

In order to expand the comparison of the software concerning the quantity projected by the Markov matrix, two new simulation models were made in the calibration process. The first one in CA_MARKOV with proportional error 0 and the other one in DINAMICA EGO with Expander option (Fig. 9). The model that bests fits with the pure Markov

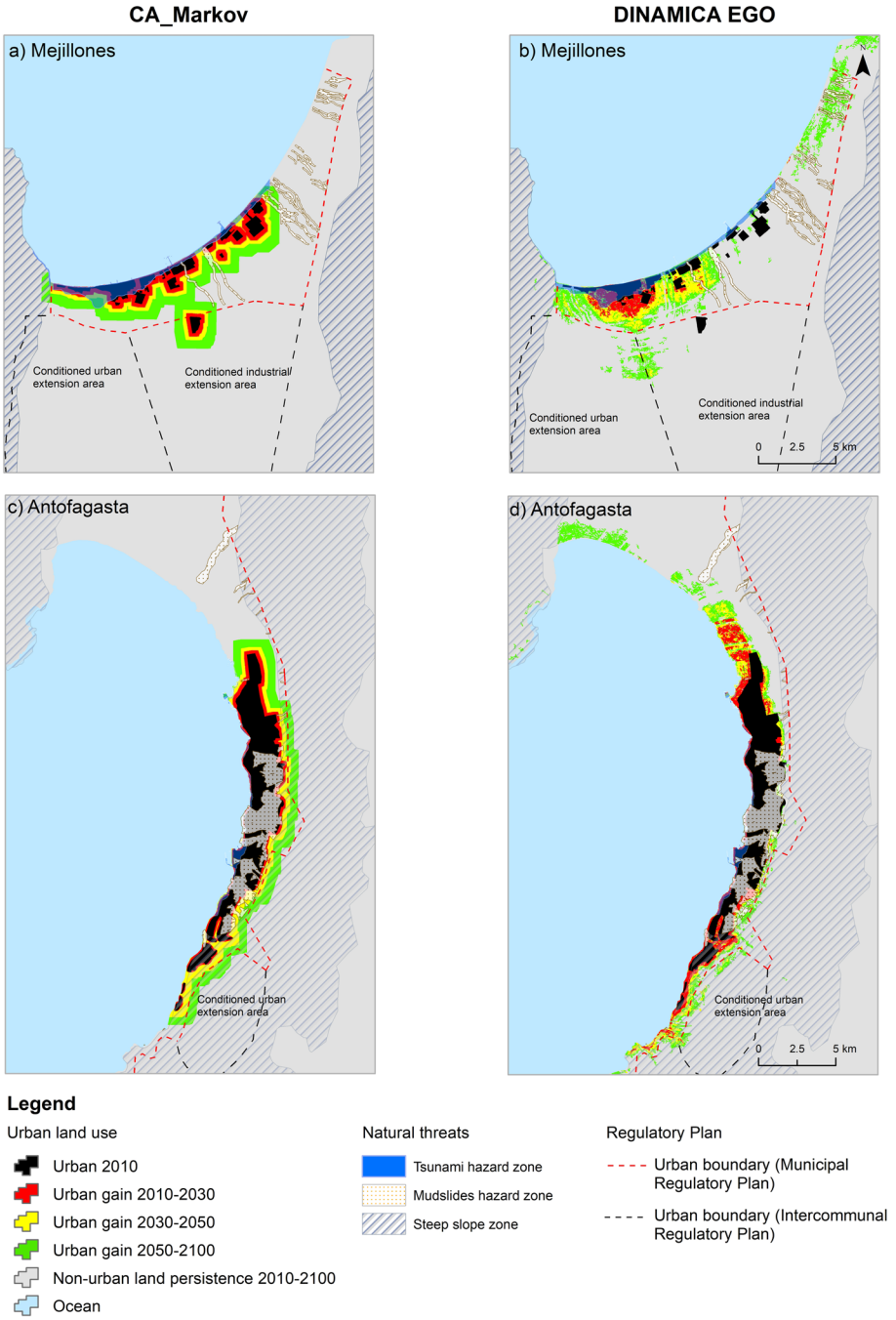

Fig. 8 Simulation of urban growth during 2010–2100 and its relationship to natural threats in Antofagasta and Mejillones

Table 3 Areas of urban exposure to natural threats (hectares) 2010–2100

Year & Model	Tsunami		Mudslide		Steep slope	
	Mejillones	Antofagasta	Mejillones	Antofagasta	Mejillones	Antofagasta
2010						
Reference	200	88	1	1,117	0	131
2030						
CA_Markov	484	187	20	3,965	0	300
DINAMICA EGO	387	198	9	4,264	6	414
2050						
CA_Markov	564	217	51	5,367	7	1056
DINAMICA EGO	432	227	28	5,103	10	698
2100						
CA_Markov	625	236	132	7,366	104	2517
DINAMICA EGO	493	234	150	6,770	58	1378

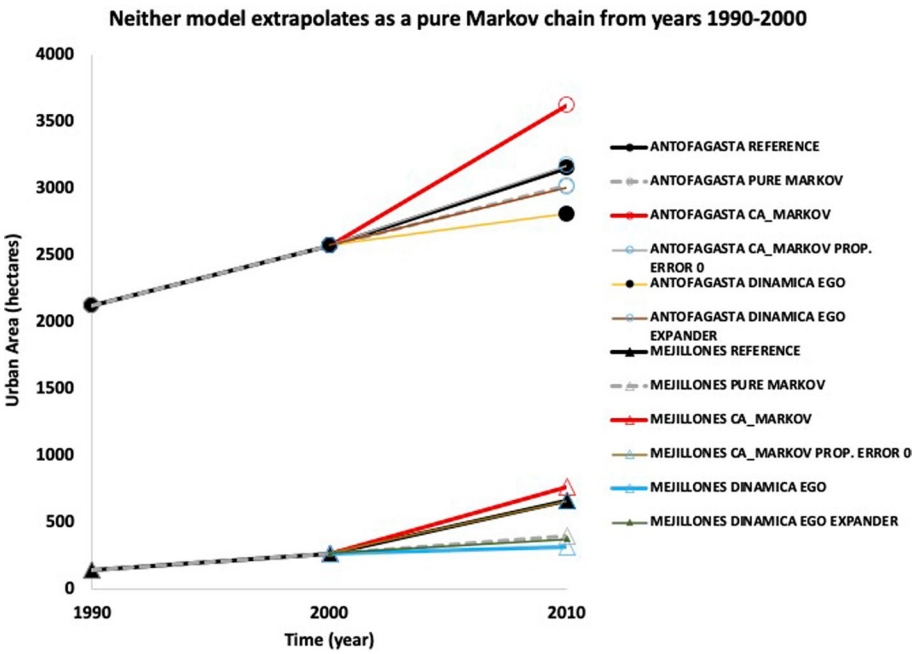

Fig. 9 Quantity of urban growth during 1990–2000 and 2000–2010 according to a pure Markov process

equation is DINAMICA EGO (Expander), with 0.4 and 4.3% quantity difference for Antofagasta and Mejillones, respectively.

Figure 10 shows the Misses, Hits, and False Alarms for each model during the validation time interval. CA_Markov predicts more urban growth than the reference urban growth in each city, thus False Alarms are greater than Misses for CA_Markov.

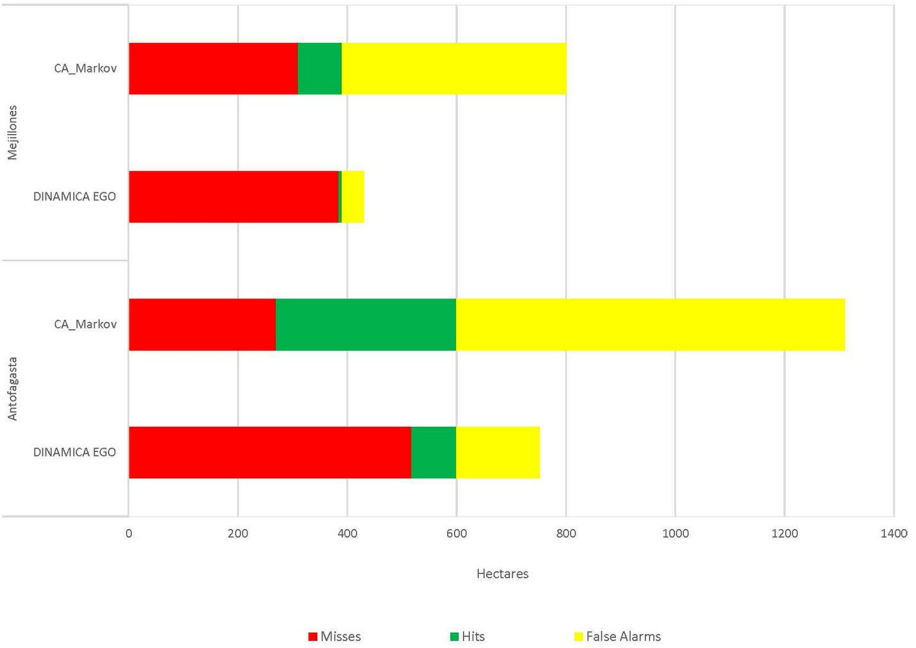

Fig. 10 Validation of urban growth during 2000–2010. Miss: observation for which diagnosis is Absence and truth is Presence for a category, also known as a False Negative and Type II error. Hit: observation for which diagnosis and truth are Presence, also known as a True Positive. False Alarm: observation for which diagnosis is Presence and truth is Absence, also known as False Positive and Type I error (Pontius Jr 2022)

DINAMICA EGO predicts less urban growth than the reference urban growth in each city, thus False Alarms are fewer than Misses for DINAMICA EGO. False Alarms are greater than Hits for all four applications, which means both models predict at wrong locations more often than at correct locations when the model simulates urban growth. CA_Markov simulates more urban growth than DINAMICA EGO thus CA_Markov has more Hits, more False Alarms, and fewer Misses than DINAMICA EGO for these particular model runs.

A popular summary metric is the Figure of Merit, which is the ratio of Hits to the sum of Misses, Hits, and False Alarms (Pontius Jr et al. 2008, 2011, 2018; Varga et al. 2019). The Figure of Merit is 10 and 25% for CA_Markov in Mejillones and Antofagasta, respectively. The Figure of Merit is 1% and 11% for DINAMICA EGO in Mejillones and Antofagasta, respectively. The Figure of Merit is a single summary metric that fails to give insight concerning whether the specification of quantity or allocation is responsible for most of the errors. The interpretation of the sizes of Misses, Hits, and False Alarms reveals that the overprediction of the quantity of urban growth causes False Alarms to be larger than Misses for CA_Markov, while the underprediction of the quantity of urban growth is responsible for False Alarms being smaller than Misses in DINAMICA EGO. Both models allow the user to modify the parameter settings for quantity separately from the parameter settings for allocation therefore the results for Figure of Merit do not imply that one model is inherently more accurate than another model. Figure 11 shows the spatial allocation of Misses, Hits, and False Alarms in each model for each city.

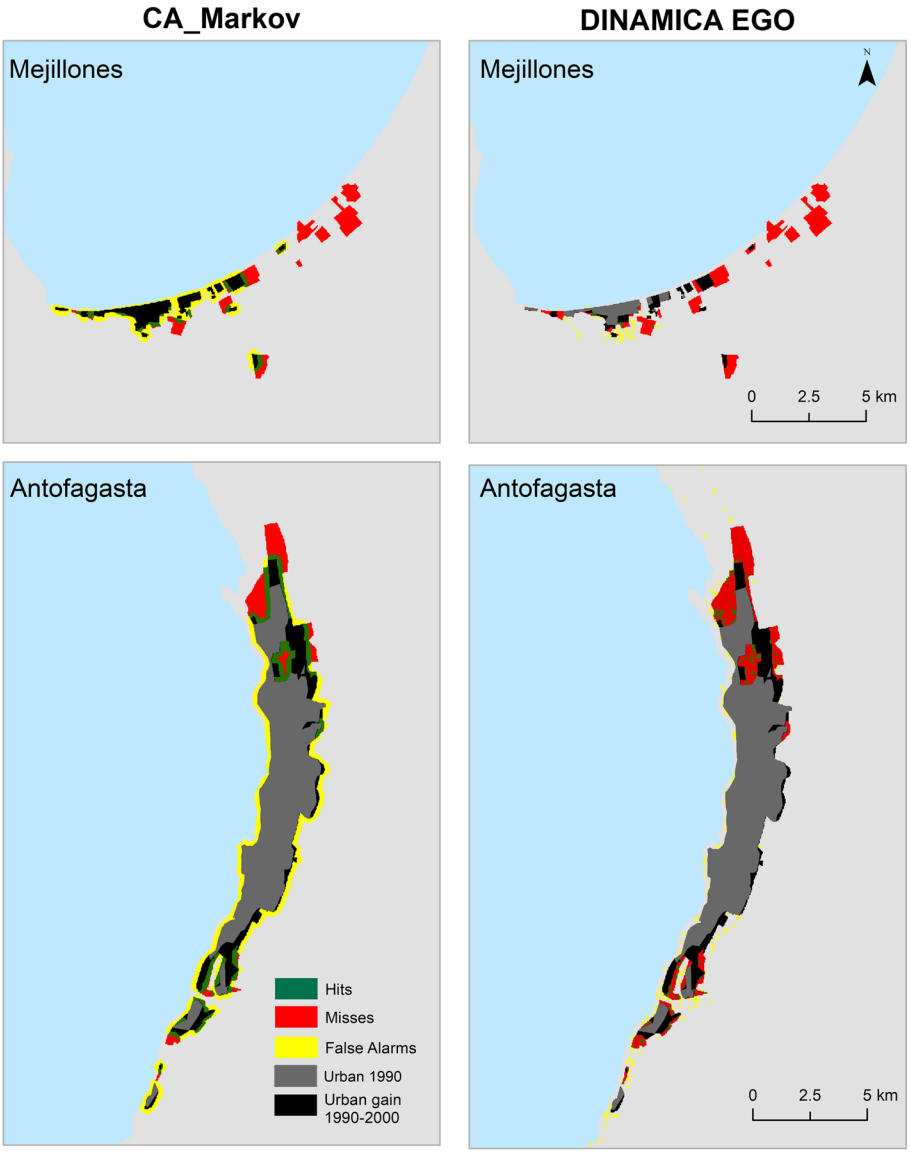

Fig. 11 Validation map for CA_Markov and DINAMICA EGO models

5 Discussion

5.1 Comparing CA_Markov and DINAMICA EGO models

According to Mas et al. (2014), the CA_Markov model has been applied to several studies such as landscape modeling (Houet and Hubert-Moy 2006), rural land use planning (Kamusoko et al. 2009), land cover prediction in Mediterranean mountains (Paegelow et al.

2008), spatial pattern changes of land use in towns and villages (Sang et al. 2011), forest cover changes (Adhikari and Southworth 2012), among others (Pontius Jr and Malanson 2005). In Chile, the model has been applied to Chillán and Los Angeles cities (Henríquez et al 2006a, b; Henríquez 2014). Viana et al. (2023) give a case study where CA_Markov simulated less change than a pure Markov chain would imply. In any case, the authors state that "cellular automata's allocation fails to follow the quantity of change that the Markov module computes" (Viana et al. 2023: 11).

DINAMICA EGO has been used mainly for studies of deforestation in the Amazon and tropical zones (Soares-Filho et al. 2002, 2006), fire regimes (Silvestrini et al. 2011), among others research related to forest degradation (Mas et al. 2014). The DINAMICA EGO model has also been applied to modeling urban growth such as the city of Bauru, west of Sao Paulo, Brazil (Almeida et al. 2005, 2003) or the metropolis of Kathmandu, Nepal (Thapa and Murayama 2011). The literature (Mas et al. 2014; Garcia-Alvarez et al. 2022) shows that the amount of land use change using Markov matrix does not show important differences between DINAMICA EGO and IDRISI (CA_Markov and Land Change Modeler).

Both models share common characteristics and some differences (Paegelow et al. 2014; Camacho et al. 2015). First, the documentation of CA_Markov and DINAMICA EGO indicates that both models use a Markov chain to determine the quantity of urban growth from the calibration time interval. Neither model followed a pure Markov chain given the parameter settings for our applications. Extrapolation assumes that the growth rates observed during the calibration period will remain the same during the simulation period, which is an erroneous assumption in many cases (Mas et al. 2014: 108). Second, CA_Markov uses heuristic MCE while DINAMICA EGO uses probabilistic WoE to determine the spatial allocation of urban growth. Third, the input of expert knowledge in the calibration stage was introduced through AHP and fuzzy process, which was the case for CA_Markov through SEREMI MINVU professional interviews. Fourth, the selection of a strong spatial filter causes CA_Markov to allocate urban growth exclusively adjacent to existing urban while our parameter settings for DINAMICA EGO caused patches of urban growth that are not connected to existing urban patches. DINAMICA EGO shows a spatial distribution more in line with the real urban pattern. For example, DINAMICA EGO projects a process of urbanization around the Juan Lopez beach town (northwest) and airport (north of Antofagasta), which in fact has grown in the last few years. Moreover, slums have grown substantially in the peripheral sectors of many Chilean cities during the most recent years. Our choice to apply a spatial filter caused CA_Markov to project urbanization near the previous urban area, while the DINAMICA EGO projects fragmented urbanization in the desert area near the coast.

Many authors have used CA_Markov and DINAMICA EGO to evaluate the impacts of future urbanization on biodiversity, agriculture, hydrology, and the atmosphere. However, we have found few applications of these models in the evaluation of natural risks. For example, the relationship between urban development modeling and the effects of the 2011 earthquake in Turkey is an interesting study that used the Cellular Automata Markov Chain (Satir et al. 2023). Young (2013) simulated the expansion of the São Paulo Metropolitan Area in relation to risk using DINAMICA EGO. A recent publication (Reimuth et al. 2024) links the future urban modeling and climate change threats, demonstrating the importance for decision-making and scientific advancement.

Some studies simulate the threats using other types of models. For example, the study by Liu et al. (2015) evaluated the interaction between the wildland–urban interface and the spatial patterns of fire risk, in Colorado, USA. Also, a study by Pathirana et al. (2014)

investigated the impact of urban growth on the changes in the extreme rainfall in and around Mumbai, India. The literature distinguishes some applications such as the TOPSIS method, which has been heuristically developed in combination with AHP techniques to deal with the problem of evaluating and prioritizing urban areas according to natural hazards but without using a spatial focus (Mahdavi et al. 2016).

5.2 Opportunities for risk management and decision-makers

The urban areas of Antofagasta and Mejillones show trends in growth towards the Atacama Desert territory that is potentially exposed to natural threats. The growth of these urban areas not only leads to an increase in the amount of surface exposure to these phenomena but also brings to the forefront threats that are not a priority in current territorial planning, as in the case of Antofagasta where landslides are associated with steep slope areas. This presents decision-makers opportunities such as the incorporation of preventive elements in the urban planning process that prevent potentially hazardous areas from being occupied by the population, as well as regularizing the construction that is in a current risk situation. In Mejillones, where there are known threats such as the danger of tsunami, this allows the most efficient management of resources and efforts to mitigate those risks.

According to this study, for the years 2030, 2050, and 2100 in Antofagasta, a part of the urbanization that is developed outside of the current urban boundary will be exposed to the threat of steep slopes. This highlights the issue that urban planning instruments can use inputs from spatially explicit model scenarios to assist risk management, especially in areas that could transform into risk zones. The need to consider these threats in land-use planning is not only necessary to prevent the new resident population and infrastructure from being exposed to these events, but also to plan safety zones, escape routes, and infrastructural roads that decrease vulnerabilities to the interior of the existing urban area. Although progress has been made in planning for climate change threats in cities in the developed world, gaps still exist between Urban Emergency Plans and Land Use Plans (Pirlone et al 2020), and the connection between future urban simulations and current and future hazard areas.

At a local level, the General Law of Urbanism and Construction approved under Decree with Force of Law 458 on April 13, 1976, defines in Article 60° that any MRP "will identify lands that are not buildable due to their special nature and location" (LGUC 1976). These non-buildable areas and risk areas are "areas restricted to urban development since they constitute a potential danger to human settlements." But frequently, these are defined without sufficient depth and without considering the urban dynamic.

At a general level, the application of both models is an important input for decision makers involved in land use planning and socio-natural risk management, especially to evaluate scenarios and reduce vulnerability. Fundamental to this is knowing if, where and how cities are growing into or into hazard-prone areas (Reimuth et al. 2024). Along with knowing how hazards will unfold in space–time. The combination of both perspectives, i.e. prospective risk assessment, is one of the main challenges for decision-makers to avoid future catastrophes (Raju et al. 2022; Reimuth et al. 2024). According Reimuth et al. (2024: 19) it is essential to consider: "(1) urban morphology patterns and potential linkages to exposure as well as vulnerability, (2) long-term time horizons to consider long-term developments, (3) feedbacks between urbanization trajectories and hazard trends, (4) the integration of future urban growth drivers and adaptation responses, (5) feedbacks between

adaptation and urbanization, and (6) scenarios, which are developed within a commonly defined scenario framework".

If urban growth simulations inspire decision-makers to stop expansive urban growth into the hazard zone, then humans might achieve more resilient and sustainable cities, especially in developing countries like Chile that are subject to extreme natural hazards.

6 Conclusions

The models allow for various behaviors concerning the simulation of the quantity and spatial allocation of landscape change. For our applications, the CA_Markov model allocates simulated urban growth near previous urban areas more so than DINAMICA EGO does. DINAMICA EGO simulates urbanization processes in the peripheric fringe, highlighting the fragmented nature that characterizes these types of cities. The use of heuristic techniques, such as the AHP and fuzzy setting process in the CA_Markov model, reflect the expert's experience in the calibration and weighting of the factors and the suitability map, to express what might be suitable for urban growth.

Spatially-explicit land change models are crucially important in the management of socio-natural risks. Most of the previous applications that we have seen are aimed toward urban scopes (transport, market, segregation, etc.) or environmental issues (loss of agricultural land, changes in runoff, degradation of biodiversity, etc.). These and other models are essential to understanding patterns, trends, and configuring scenarios for land planning and risk management in fast-growing cities.

Author contributions The authors contributed to the study conception and design. Material preparation, data collection, fieldwork, analysis and written were performed by Cristian Henriquez. Paulina Contreras assisted with data modeling, validation, and mapping. Robert Gilmore Pontius Jr has contributed to the conceptualization of the models.

Funding This study has been funded by Fondo Nacional de Desarrollo Científico y Tecnológico, Fondecyt/ANID Project No. 1220688. The authors gratefully acknowledge the research support provide by CIGIDEN, ANID FONDAP N° 1523A0009, CEDEUS, ANID FONDAP No. 1523A0004, and The United States National Science Foundation supported this research through its Long Term Ecological Research network via grants OCE-1637630 and OCE-2224608. We thank Andrés Romero, and Milena Sanabria, who assisted in collecting, and processing data.

Declarations

Conflict of interest The authors have no relevant financial or non-financial interests to disclose.

References

Adhikari S, Southworth J (2012) Simulating forest cover changes of Bannerghatta National Park based on a CA-Markov Model: a remote sensing approach. Remote Sens 4(10):3215–3243. https://doi.org/10.3390/rs4103215

Agarwal C, Green G, Grove J, Evans TP, Schwei, CM (2002) A review and assessment of land-use change models: dynamics of space, time, and human choice. United States Department of Agriculture Forest Service, General Technical Report NE-297, Indiana University

Almeida C, Batty M, Monteiro M, Câmara G, Soares-Filho BS, Cerqueira G, Pennachin C (2003) Stochastic cellular automata modeling of urban land use dynamics: empirical development and estimation. Comput Environ Urban Syst 27:481–509

Almeida CM, Monteiro AMV, Soares-Filho BS, Cerqueira GC, Pennachin C, Batty M (2005) GIS and remote sensing as tools for the simulation of urban land-use change. Int J Remote Sens 26(4):759–774

Barrett BS, Campos DA, Vicencio Veloso J, Rondanelli R (2016) Extreme temperature and precipitation events in March 2015 in central and northern Chile. J Geophys Res—Atmos 121:4563–4580. https://doi.org/10.1002/2016JD024835

Barrientos S (2014) Informe Técnico Terremoto de Iquique, Mw = 8.2 (p. 19). Centro Sismológico Nacional Universidad de Chile, Santiago

Béjar-Pizarro M, Socquet A, Armijo R, Carrizo D, Genrich J, Simons M (2013) Andean structural control on interseismic coupling in the North Chile subduction zone. Nat Geosci 6(6):462–467. https://doi.org/10.1038/ngeo1802

Bozzolan E, Holcombe E, Pianosi F, Wagener T (2020) Including informal housing in slope stability analysis - an application to a data-scarce location in the humid tropics. Nat Hazard 20(11):3161–3177. https://doi.org/10.5194/nhess-20-3161-2020

Camacho MT, Pontius RG Jr, Paegelow M, Mas J-F (2015) Comparison of simulation models in terms of quantity and allocation of land change. Environ Model Softw 69:214–221

Chen K, Blong R, Jacobson C (2001) MCE-RISK: Integrating multicriteria evaluation and GIS for risk decision-making in natural hazards. Environ Model Softw. https://doi.org/10.1016/S1364-8152(01)00006-8

Clark Labs (2012) Idrisi Selva Tutorial. Clark Labs, Clark University, Worcester. http://www.clarklabs.org/products/idrisi.cfm

Dekkers J, Rietveld P (2011) Explaining land-use transition in a segmented land market. In: Koomen E, Borsboom-van Beurden J (eds) Land-use modelling in planning practice. Springer, Dordrecht, Heidelberg, London, New York

Depicker A, Jacobs L, Mboga N, Smets B, Van Rompaey A, Lennert M et al (2021) Historical dynamics of landslide risk from population and forest-cover changes in the Kivu Rift. Nat Sustain 4(11):965–974. https://doi.org/10.1038/s41893-021-00757-9

Dille A, Dewitte O, Handwerger AL, D'Oreye N, Derauw D, Bamulezi GG et al (2022) Acceleration of a large deep-seated tropical landslide due to urbanization feedbacks. Nat Geosci 15(12):1048. https://doi.org/10.1038/s41561-022-01073-3

Ferreira ME, Ferreira LG, Miziara F, Soares-Filho BS (2013) Modeling landscape dynamics in the central Brazilian savanna biome: future scenarios and perspectives for conservation. J Land Use Sci 8(4):403–421. https://doi.org/10.1080/1747423X.2012.675363

Garcia-Alvarez D (2018) The influence of scale in LULC modeling. a comparison between two different LULC maps (SIOSE and CORINE). In: Camacho Olmedo MT, Paegelow M, Mas J-F, Escobar F (eds) Geomatic approaches for modeling land change scenarios, series: lecture notes in geoinformation and cartography. Springer, Cham, pp 187–213. https://doi.org/10.1007/978-3-319-60801-3_10

Garcia-Alvarez D, Olmedo MTC, Van Delden H, Mas JF (2022) Comparing the structural uncertainty and uncertainty management in four common Land Use Cover Change (LUCC) model software packages. Environ Modell Softw. https://doi.org/10.1016/j.envsoft.2022.105411

Garreaud R, Rutllant J (1996) Análisis meteorológico de los aluviones de Antofagasta y Santiago de Chile en el periodo 1991–1993. Atmósfera 9(4):251–271

Hauser A (1997) Los aluviones del 18 de junio de 1991 en Antofagasta: un análisis crítico, a 5 años del desastre. Servicio Nacional de Geología y Minería, Chile. Boletín No. 49

Hayes GP, Herman MW, Barnhart WD, Furlong K, Riquelme S, Benz HM, Samsonov S (2014) Continuing megathrust earthquake potential in Chile after the 2014 Iquique earthquake. Nature 512(7514):295–298. https://doi.org/10.1038/nature13677

Henríquez C, Azócar G, Aguayo M (2006a) Cambio de uso del suelo y escorrentía superficial: aplicación de un modelo de simulación espacial en Los Ángeles, VIII Región del Biobío. Chile Rev Geograf Norte Grande 36:61–74. https://doi.org/10.4067/S0718-34022006000200004

Henríquez C, Azócar G, Romero H (2006b) Monitoring and modeling the urban growth of two mid-sized Chilean cities. Habitat Int 30(4):945–964. https://doi.org/10.1016/j.habitatint.2005.05.002

Henríquez C, Qüense J, Villarroel C, Mallea C (2019) 50-years of climate extreme indices trends and inventory of natural disasters in Chilean Cities (1965–2015). In: Henríquez C, Romero H (eds) Urban climates in Latin America. Springer, Dordrecht, pp 281–308

Henríquez C (2014) Modelando el crecimiento de ciudades medias. Hacia un desarrollo urbano sustentable. Ediciones UC, Colección Textos Universitarios, Santiago, 314pp

Houet T, Hubert-Moy L (2006) Modelling and projecting land-use and land-cover changes with a cellular automaton considering landscape trajectories: an improvement for simulation of plausible future states. EARSeL eProc 5:63–76

Huong HTL, Pathirana A (2013) Urbanization and climate change impacts on future urban flooding in Can Tho city. Vietnam Hydrol Earth Syst Sci 17(1):379–394. https://doi.org/10.5194/hess-17-379-2013

Ilustre Municipalidad de Antofagasta (2012) Plano Seccional de Avenida Cerro Paranal (Sector Angamos)

Ilustre Municipalidad de Mejillones (2013) Plano Regulador Comunal

Instituto Nacional de Estadísticas Chile—INE (2018) Síntesis de resultados censo 2017. Instituto Nacional de Estadística (INE), Santiago. http://www.censo2017.cl/descargas/home/sintesis-de-resultados-censo2017.pdf

Instituto Nacional de Estadísticas, Región de Antofagasta—INE (2013) Estadísticas de medio ambiente región de Antofagasta. http://www.ineantofagasta.cl/contenido.aspx?id_contenido=134. Accessed 17 Oct 2014

Jacobs C, Bouwman A, Koomen E, van der Burg A (2011) Lessons learned from using land-use simulation in regional planning. In: Koomen E, Borsboom-van Beurden J (eds) Land-use modelling in planning practice. Springer, Dordrecht, Heidelberg, London, New York

Kamusoko C, Aniya M, Adi B, Manjoro M (2009) Rural sustainability under threat in Zimbabwe e Simulation of future land use/cover changes in the Bindura district based on the Markov-cellular automata model. Appl Geogr 29:435–447

Kuijpers-Linde M (2011) A policy perspective of the development of Dutch land-use models. In: Koomen E, Borsboom-van Beurden J (eds) Land-use modelling in planning practice. Springer, Dordrecht, Heidelberg, London, New York

La Red / DesInventar (2009) DesInventar Sistema de Inventario de Desastres. Corporación OSSO, Red de Estudios Sociales en Prevención de Desastres: http://online.desinventar.org/desinventar/#CHL-1257983285-chile_inventario_historico_de_desastres

Ley General de Urbanismo y Construcciones—LGUC (1976) Decreto con Fuerza de Ley 458. Publication date April 13, 1976 (Decree 67, Ministry of Housing and Urban Planning)

Liu Y, Feng Y, Pontius RG Jr (2014) Spatially-explicit simulation of urban growth through self-adaptive genetic algorithm and cellular automata modelling. Land 3(3):719–738. https://doi.org/10.3390/land3030719

Liu Z, Wimberly MC, Lamsal A, Sohl TL, Hawbaker TJ (2015) Climate change and wildfire risk in an expanding wildland–urban interface: a case study from the Colorado Front Range Corridor. Landscape Ecol 30:1943–1957

Mahdavi R, Ramesht MH, Ghazi I, Khajedin SK, Seif A, Nohegar A, Mahdavi A (2016) Identification of natural hazards and classification of urban areas by TOPSIS model (case study: Bandar Abbas city, Iran) *Geomatics*. Nat Hazards Risk 7(1):85–100

Mahiny A, Clarke K (2012) Guiding SLEUTH land-use/land-cover change modeling using multicriteria evaluation: towards dynamic sustainable land-use planning. Environ Plann B Plann Des 39:925–944

Martins VN, Cabral P, Sousa SD (2012) Urban modelling for seismic prone areas: the case study of Vila Franca do Campo (Azores Archipelago, Portugal). Nat Hazards Earth Syst Sci 12:2731–2741

Mas JF, Pérez-Vega A, Clarke KC (2012) Assessing simulated land use/cover maps using similarity and fragmentation indices. Ecol Complex 11:38–45. https://doi.org/10.1016/j.ecocom.2012.01.004

Mas JF, Kolb M, Paegelow M, Camacho MT, Houet T (2014) Inductive pattern-based land use/cover change models: a comparison of four software packages. Environ Model Softw 5:94–111

McGarigal K, Cushman SA, Ene E (2015) FRAGSTATS v4: Spatial pattern analysis program for categorical maps. Computer software program produced by the authors; available at the following web site: https://www.fragstats.org

National Research Council (2014) Advancing land change modeling: opportunities and research requirements. National Academies Press, Washington [Web.] Retrieved from the Library of Congress. https://lccn.loc.gov/2015452065

NOAA Center for Weather and Climate Prediction (2014) Historical El Nino/La Nina episodes (1950-present). http://www.cpc.noaa.gov/products/analysis_monitoring/ensostuff/ensoyears.shtml. Accessed 17 Oct 2014

ONEMI (2015a) Análisis multisectorial eventos 2015. Evento Hidrometeorológico Marzo—Terremoto/Tsunami, Septiembre. Comité Científico Técnico, Oficina Nacional de Emergencia, Santiago de Chile. http://repositoriodigitalonemi.cl/web/bitstream/handle/2012/1744/Informe_CCT_2015_AnalisisEventos.pdf?sequence=1

ONEMI (2015b) Monitoreo por evento hidrometeorológico. Oficina Nacional de Emergencia, Santiago de Chile. http://www.onemi.cl/alerta/monitoreo-por-evento-hidrometeorologico/

Ozturk U, Bozzolan E, Holcombe EA, Shukla R, Pianosi F, Wagener T (2022) How climate change and unplanned urban sprawl bring more landslides. Nature 608(7922):262–265. https://doi.org/10.1038/d41586-022-02141-9

Paegelow M, Camacho Olmedo MT, Ferraty F, Ferré L, Sarda P, Villa N (2008) Prospective modelling of environmental dynamics. A methodological comparison applied to mountain land cover changes. In: Paegelow M, Camacho Olmedo MT (eds) Modelling environmental dynamics advances in geomatic solutions, series: environmental science and engineering. Springer, Berlin, Heidelberg, pp 141–168

Paegelow M, Camacho Olmedo MT, Mas JF, Houet T (2014) Benchmarking of LUCC modelling tools by various validation techniques and error analysis. Cybergeo. https://doi.org/10.4000/cybergeo.26610. http://cybergeo.revues.org/26610

Pararas-Carayannis G (2010) The Earthquake and Tsunami of 27 February 2010 in Chile–evaluation of source mechanism and of near and far-field tsunami effects. Science of Tsunami Hazards. http://agris.fao.org/agris-search/search/display.do?f=2012/DJ/DJ2012089300586.xml;DJ2012089394

Pathirana A, Denekew HB, Veerbeek W, Zevenbergen C, Banda AT (2014) Impact of urban growth-driven landuse change on microclimate and extreme precipitation—a sensitivity study. Atmos Res 138:59–72

Pérez-Vega A, Mas JF, Ligmann-Zielinska A (2012) Comparing two approaches to land use/cover change modeling and their implications for the assessment of biodiversity loss in a deciduous tropical forest. Environ Model Softw 29(1):11–23. https://doi.org/10.1016/j.envsoft.2011.09.011

Pijanowski BC, Brown DG, Shellito B, Manik G (2002) Using neural networks and GIS to forecast land use changes: a Land Transformation Model. Comput Environ Urban Syst 26(6):553–575. https://doi.org/10.1016/S0198-9715(01)00015-1

Pirlone F, Spadaro I, Candia S (2020) More resilient cities to face higher risks. The case of Genoa. Sustainability (switzerland). https://doi.org/10.3390/SU12124825

Pontius RG Jr (2022) Metrics that make a difference How to analyze change and error, series: advances in geographic information science, vol 117. Springer Nature, Cham. https://doi.org/10.1007/978-3-030-70765-1

Pontius RG Jr, Malanson J (2005) Comparison of the structure and accuracy of two land change models. Int J Geogr Inf Sci 19(2):243–265. https://doi.org/10.1080/13658810410001713434

Pontius RG Jr, Boersma W, Castella JC, Clarke K, Nijs T, Dietzel C, Duan Z, Fotsing E, Goldstein N, Kok K, Koomen E, Lippitt CD, McConnell W, Sood AM, Pijanowski B, Pithadia S, Sweeney S, Trung TN, Veldkamp AT, Verburg PH (2008) Comparing the input, output, and validation maps for several models of land change. Ann Reg Sci 42(1):11–37. https://doi.org/10.1007/s00168-007-0138-2

Pontius RG Jr, Peethambaram S, Castella JC (2011) Comparison of three maps at multiple resolutions: A case study of land change simulation in Cho Don district, Vietnam. Ann Assoc Am Geogr. https://doi.org/10.1080/00045608.2010.517742

Pontius RG Jr, Castella JC, de Nijs T, Duan Z, Fotsing E, Goldstein N, Kok K, Koomen E, Lippitt CD, Mcconnell W, Mohd Sood A, Pijanowski B, Verburg P, Veldkamp AT (2018) Lessons and challenges in land change modeling derived from synthesis of cross-case comparisons. In: Behnisch M, Meinel G (eds) Trends in spatial analysis and modelling, vol 19. Springer, New York, pp 143–164. https://doi.org/10.1007/978-3-319-52522-8_8

Pozoukidou G (2014) Land use transport interaction models: application perspectives for the city of Thessaloniki. Spatium 32:7–14

Pritchard M, Simons M (2002) Co-seismic slip from the 1995 July 30 Mw = 8.1 Antofagasta, Chile, earthquake as constrained by InSAR and GPS observations. Geophys J Int 362–376

Puertas OL, Henríquez C, Meza FJ (2014) Assessing spatial dynamics of urban growth using an integrated land use model. Application in Santiago Metropolitan Area, 2010–2045. Land Use Policy 38:415–425. https://doi.org/10.1016/j.landusepol.2013.11.024

Raju E, Boyd E, Otto F (2022) Stop blaming the climate for disasters Comment. Commun Earth Environ. https://doi.org/10.1038/s43247-021-00332-2

Reimuth A, Hagenlocher M, Yang LM, Katzschner A, Harb M, Garschagen M (2024) Environ Res Lett 19:013002. https://doi.org/10.1088/1748-9326/ad1082

Saaty TL (1980) The analytic hierarchy process. McGraw Hill, New York

Sang L, Zhang C, Yang J, Zhu D, Yun W (2011) Simulation of land use spatial pattern of towns and villages based on CA e Markov model. Math Comput Model 54:938–943

Sarricolea P, Herrera MJ, Mesenguer O (2017) Climatic regionalisation of continental Chile. J Maps 13:66–73

Satir O, Kemec S, Yeler O, Akin A, Bostan P, Ersoy Mirici M (2023) Simulating the impact of natural disasters on urban development in a sample of earthquake. Nat Hazards 116:3839–3855. https://doi.org/10.1007/s11069-023-05838-w

Schurr B, Asch G, Hainzl S, Bedford J, Hoechner A, Palo M, Wang R, Moreno M, Bartsch M, Zhang Y, Oncken O, Tilmann F, Dahm T, Victor P, Barrientos S, Vilotte JP (2014) Gradual unlocking of plate boundary controlled initiation of the 2014 Iquique earthquake. Nature 512(7514):299–302. https://doi.org/10.1038/nature13681

SEREMI MINVU (2004) Plan regulador intercomunal del borde costero de la II región. Regional Secretariat of the Ministry of Housing and Urban Planning of Antofagasta
Servicio Hidrográfico y Oceanográfico de la Armada de Chile (2012) Carta de Inundación por Tsunami, Mejillones, p 1
Servicio Hidrográfico y Oceanográfico de la Armada de Chile—SHOA (2013) Carta de Inundación por Tsunami, Antofagasta —Coloso
Silvestrini RA, Soares-Filho BS, Nepstad D, Coe M, Rodrigues HO, Assunção R (2011) Simulating fire regimes in the Amazon in response to climate change and deforestation. Ecol Appl 21(5):1573–1590
Soares-Filho BS, Cerqueira G, Pennachin C (2002) Dinamica-a stochastic cellular automata model designed to simulate the landscape dynamics in an Amazonian colonization frontier. Ecol Model 154(3):217–235. https://doi.org/10.1016/S0304-3800(02)00059-5
Soares-Filho BS, Nepstad D, Curran L, Voll E, Cerqueira G, Garcia RA, Ramos CA, McDonald A, Lefebvre P, Schlesinger P (2006) Modeling conservation in the Amazon basin. Nature 440:520–523
Soares-Filho BS, Rodrigues H, Costa W (2009) Modeling environmental dynamics with dinamica EGO In: Soares-Filho BS, Rodrigues H, Souza Costa WL 2ed (2010). Belo Horizonte, 120p. ISBN: 978-85-910119-0-2
Thapa RB, Murayama Y (2011) Urban growth modeling of Kathmandu metropolitan region. Nepal Comput Environ Urban Syst 35(1):25–34
Trentin G, Isabel M, Freitas CD (2010) Modelagem da dinâmica espacial urbana: modelo de autômato celular na simulação de cenários para o Município de Americana, pp 291–305
United Nations (2019) World urbanization prospects: the 2018 revision. New York
Varga OG, Pontius RG Jr, Sing SK, Szabó S (2019) Intensity analysis and the figure of Merit's components for assessment of a cellular automata—Markov simulation model. Ecol Ind 101:933–942
Vargas G, Ortlieb L, Rutllant J (2000) Aluviones históricos en Antofagasta y su relación con eventos El Niño/Oscilación del sur. Rev Geol Chile 27(2):157–176. https://doi.org/10.4067/S0716-02082000000200002
Vargas G, Ortlieb L (1997) Registro de aluviones históricos en Antofagasta. In: Congreso geológico Chileno, Actas, vol 1, pp 400–404
Veerbeek W, Denekew H (2011) Urban growth modeling to predict the changes in the urban microclimate and urban water cycle. Int Confer Urban Drain 1–8
Viana CM, Pontius RG Jr, Rocha J (2023) Four fundamental questions to evaluate land change models with an illustration of a Cellular Automata—Markov model. Ann Am Assoc Geogr. https://doi.org/10.1080/24694452.2023.2232435
Waddell P (2011) Integrated land use and transportation planning and modelling: addressing challenges in research and practice. Transp Rev 31(2):209–229. https://doi.org/10.1080/01441647.2010.525671
Weber C, Puissant A (2003) Urbanization pressure and modeling of urban growth: example of the Tunis Metropolitan Area. Remote Sens Environ 86(3):341–352. https://doi.org/10.1016/S0034-4257(03)00077-4
Weng Q (2001a) A remote sensing-GIS evaluation of urban expansion and its impact on surface temperature in the Zhujiang Delta, China. Int J Remote Sens 22(10):1999–2014. https://doi.org/10.1080/713860788
Weng Q (2001b) Modeling urban growth effects on surface runoff with the integration of remote sensing and GIS. Environ Manage 28(6):737–748. https://doi.org/10.1007/s002670010258
Wilcox AC, Escauriaza C, Agredano R, Mignot E, Zuazo V, Otárola S, Castro L, Gironás L, Cienfuegos R, Mao L (2016) An integrated analysis of the March 2015 Atacama floods. Geophys Res Lett 43:8035–8043. https://doi.org/10.1002/2016GL069751
Young AF (2013) Urban expansion and environmental risk in the São Paulo Metropolitan Area. Clim Res 57(1):73–80. https://doi.org/10.3354/cr01161
Zerger A (2002) Examining GIS decision utility for natural hazard risk modelling. Environ Model Softw 17(3):287–294. https://doi.org/10.1016/S1364-8152(01)00071-8

Publisher's Note Springer Nature remains neutral with regard to jurisdictional claims in published maps and institutional affiliations.

Springer Nature or its licensor (e.g. a society or other partner) holds exclusive rights to this article under a publishing agreement with the author(s) or other rightsholder(s); author self-archiving of the accepted manuscript version of this article is solely governed by the terms of such publishing agreement and applicable law.